

A Simultaneous ASCA and RXTE Long Look at the Seyfert 1 Galaxy MCG-6-30-15

J. C. Lee, A. C. Fabian, and K. Iwasawa

Institute of Astronomy; Madingley Road; Cambridge CB3 0HA UK

W. N. Brandt

Department of Astronomy and Astrophysics; The Pennsylvania State University; 525 Davey Lab; University Park, PA 16802 USA

C. S. Reynolds

JILA; Campus Box 440; University of Colorado; Boulder, 80309-0440 USA

Abstract. We report on a joint RXTE and ASCA observation spanning ~ 400 ks of the Seyfert 1 galaxy MCG-6-30-15. The low energy coverage of ASCA coupled with the high energy coverage of RXTE have allowed us not only to confirm features of Compton reflection but also to set bounds on the abundances as a function of reflective fraction.

1. Introduction

The current paradigm for AGN is a central engine consisting of an accretion disk surrounding a supermassive black hole (e.g. see review by Rees 1984). The main source of power is the release of gravitational potential energy as matter falls towards the central black hole. Much of this energy is released in the form of X-rays, some fraction of which are reprocessed by matter in the AGN.

Careful study of X-ray reprocessing mechanisms can give much information about the immediate environment of the accreting black hole. These effects of reprocessing can often be observed in the form of emission and absorption features in the X-ray spectra of AGNs. In Seyfert 1 nuclei, approximately half of the X-rays are *reflected* off the inner regions of the accretion disk. The reflected spectrum is complicated with features of photoabsorption, iron fluorescence and Compton scattering (George & Fabian 1991). The strength, shape and broadening of the features of the reflected spectrum are diagnostics of the geometry, ionization state, and iron abundance of the accretion disk.

MCG-6-30-15 is a Seyfert 1 galaxy that is both bright and nearby ($z = 0.008$). The spectral features above a few keV can be modeled well by a power-law continuum plus reflection component that encompasses the effects of reflection of this continuum by the inner regions of the accretion disk. The principle observables of this reflection component are a strong iron fluorescence line at ~ 6.4 keV and a Compton ‘hump’ peaking at 20–30 keV. The iron line together with the reflection component are important diagnostics for the geometry and

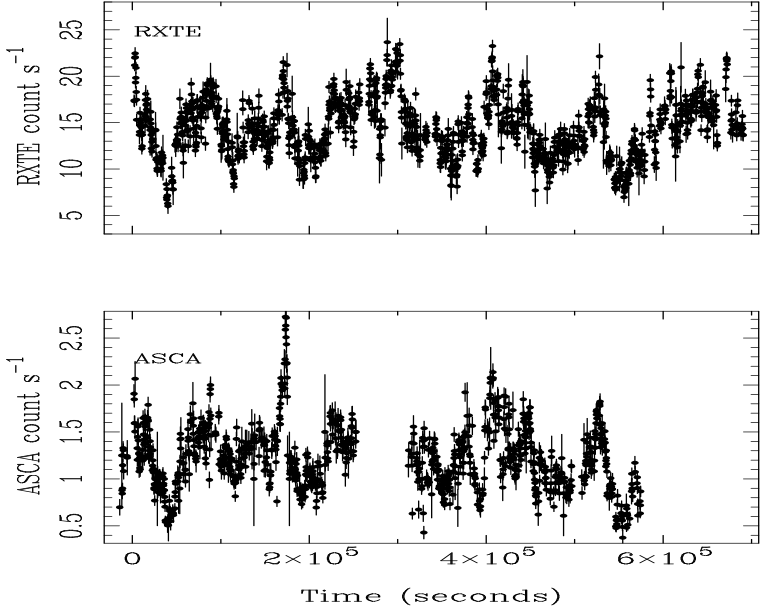


Figure 1. MCG-6-30-15 was observed simultaneously by RXTE and ASCA spanning ~ 400 ks over the period from 1997 August 3 to 1997 August 12. The RXTE on-source time was ~ 400 ks and the ASCA on-source time was ~ 200 ks.

physics of the X-ray continuum source. The strength of the emission line relative to the reflection hump depends largely on the abundance of iron relative to hydrogen in the disk. Disentangling the abundance from the absolute normalization of the reflection component is an important step in constraining physical models of AGN central regions.

Previous studies of Ginga spectra have suggested that the reflection component is present in many Seyfert 1 AGNs (Nandra & Pounds 1994). Our recent observations using the Rossi X-ray Timing Explorer (RXTE) have clearly confirmed the presence of reflection in MCG-6-30-15.

2. Observations

MCG-6-30-15 was observed by RXTE for 400 ks over the period from 1997 August 4 to 1997 August 12 by both the Proportional Counter Array (PCA) and High-Energy X-ray Timing Experiment (HEXTE) instruments. It was simultaneously observed by the Advanced Satellite for Cosmology and Astrophysics (ASCA) Solid-state Imaging Spectrometers (SIS) for 200 ks over the period 1997 August 3 to 1997 August 10 with a half-day gap in the middle. We concentrate primarily on the RXTE observation.

PCA light curves and spectra are extracted from only the top Xenon layer using the FTOOLS v.4.0 software. We use only combined data from PCUs 0, 1,

and 2 since PCUs 3 and 4 are sometimes turned off due to occasional problems with discharge. Good time intervals were selected to exclude any Earth or South Atlantic Anomaly (SAA) passage occultations, and to ensure stable pointing.

We generate background data using PCABACKEST v2.0C in order to estimate the internal background caused by interactions between the radiation/particles and the detector/spacecraft at the time of observation. This is done by matching the conditions of observations with those in various model files. The model files that we chose were constructed using the VLE rate (one of the rates in PCA Standard 2 science array data that is defined to be the rate of events which saturate the analog electronics) as the tracer of the particle background.

The PCA response matrix for the RXTE data set was provided by the RXTE Guest Observer Facility (GOF) at Goddard Space Flight Center. Background models and response matrices are representative of the most up-to-date PCA calibrations.

The net HEXTE spectra were generated by subtracting spectra from the off-source positions from the on-source data. Time intervals were chosen to exclude 30 seconds prior to and following SAA passages. This avoids periods when the internal background is changing rapidly. We use response matrices provided by the HEXTE team at the University of California, San Diego. The relative normalizations of the PCA and the two HEXTE clusters are allowed to vary, due to uncertainties (< about 5%) in the HEXTE deadtime measurement.

ASCA data reduction was carried out using FTOOLS version 4.0 and 4.1 with standard calibration provided by the ASCA GOF. Detected SIS events with a grade of 0, 2, 3 or 4 are used for the analysis. One of the standard data selection criteria, BR EARTH, elevation angle of the source from the bright Earth rim, is found to affect little the soft X-ray data from the SIS. We thus use the SIS data of approximately 231 ks from each detector for spectral analysis. The source counts are collected from a region centred at the X-ray peak within ≈ 4 arcmin from the SIS and 5 arcmin from the GIS. The background data are taken from a (nearly) source-free region in the same detector with the same observing time.

Figure 1 shows the ASCA S0 160-2700 pha-channel (≈ 0.6 –10 keV), and the RXTE PCA 1–129 pha channel (≈ 2 –60 keV) background subtracted light curves. There is a gap of ~ 60 ks in the ASCA light curve in which the satellite observed IC4329A while MCG–6–30–15 underwent a large flare observed by RXTE. Significant variability can be seen in both light curves on short and long timescales. Flare and minima events are seen to correlate temporally in both light curves.

3. Spectral Fits

We restrict ASCA and PCA data analysis to be respectively between 3–10 keV and 3–20 keV (the PCA on-source spectrum for MCG–6–30–15 is largely background dominated past 20 keV). The lower energy restriction at 3 keV is selected in order that the necessity for modeling photoelectric absorption due to Galactic ISM material, or the warm absorber that is known to be present in this object (i.e. Reynolds et al. 1995) is removed. HEXTE data is restricted to be between 16 and 50 keV in order that we may adequately model the reflection hump. We also include 0.5 per cent systematics to the PCA data.

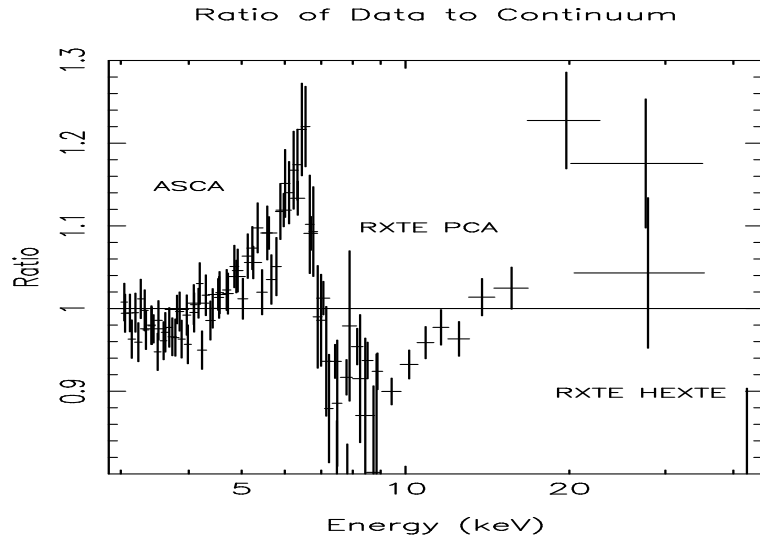


Figure 2. A *nominal* fit using a simple power-law demonstrates the clear existence of a redshifted broad iron line at ~ 6.0 keV and reflection component above 10 keV.

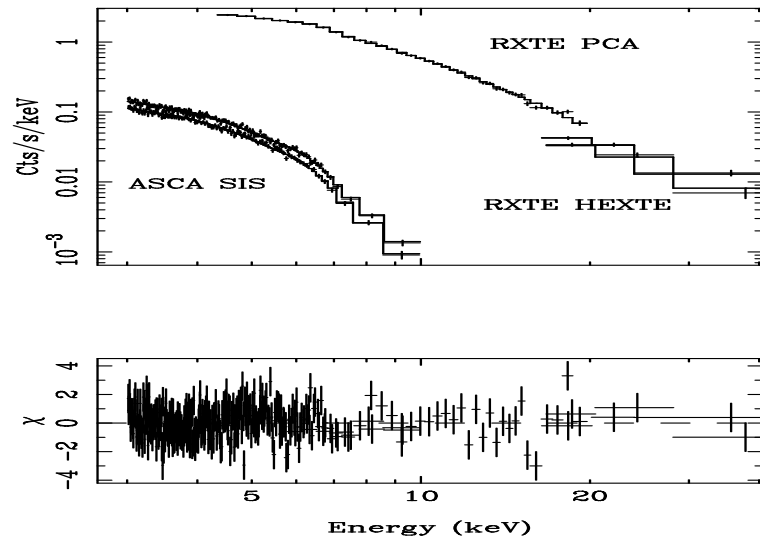


Figure 3. A multicomponent model fit that includes the reflected spectrum to all three data sets (i.e. ASCA, RXTE PCA and HEXTE) shows that the residuals are essentially flat.

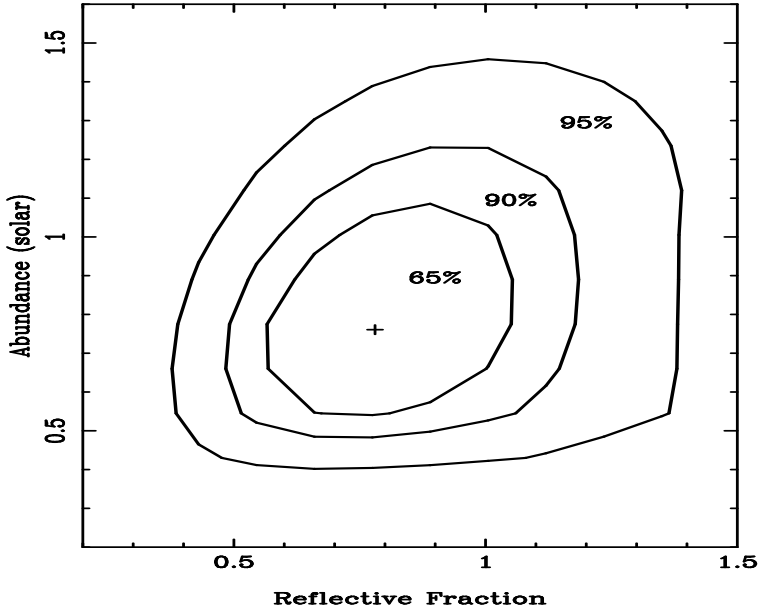


Figure 4. RXTE PCA+HEXTE 65, 90, and 95 per cent confidence contours for the relationship between abundances and reflective fraction. The energy range of fit is between 3 and 50 keV.

3.1. Spectral Features

A *nominal* fit using a simple power law confirms the clear existence of a redshifted broad iron line at ~ 6.0 keV and reflection component above 10 keV as shown in Lee et al. (1998, in press). A plot of the ratio of data to continuum shown in figure 2 demonstrates the significance of these features.

As further evidence for the existence of the reflection component and good agreement between ASCA and RXTE, figure 3 shows that the residuals are essentially flat when all three data sets (i.e. ASCA, RXTE PCA + HEXTE) are fit with a multicomponent model. This model consists of a power-law reflection component (Magdziarz & Zdziarski 1995) to model the primary and reflected continuum with an additional Gaussian component to represent the iron K α emission. Fitting the RXTE data in the energy range 3–50 keV we obtain for a best fit power-law slope $\Gamma = 2.05^{+0.13}_{-0.06}$. The line energy is $5.94^{+0.15}_{-0.19}$ keV, with line width $\sigma = 0.62^{+0.20}_{-0.25}$ keV. The equivalent width $EW = 305^{+6}_{-19}$ eV, and the reduced- χ^2 for the overall fit is 0.51 for 48 degrees of freedom.

The improved S/N (as compared to GINGA) along with the broad waveband coverage afforded by RXTE has allowed us not only to detect features associated with Compton reflection but also to set bounds on the abundances as a function of reflective fraction. Figure 4 shows that 95 per cent confidence contours can be obtained by fitting in the energy range 3–50 keV, with best fit values for reflective fraction and lower elemental abundances set equal to that

of iron respectively to be 0.78 ± 0.31 and $0.76^{+0.33}_{-0.29}$ solar abundances. The reflective fraction is defined such that its value equal to unity implies that the X-ray source is subtending 2π sr of the sky (i.e. $\frac{\Omega}{2\pi} = 1$).

In order to test the consistency of our results, we perform fits similar to those above on an ~ 187 ks subset (from the first portion) of the RXTE observation, and find that results are nearly identical. This gives us confidence that our derived parameters have physical meaning. Implications of the large EW of the iron line will be addressed in future publications.

4. Summary

Previous studies of reflection of X-rays from optically thick cold matter in the central region of AGNs have concluded that a reflected spectrum exists and is observed above the primary continuum. However, most studies in the past have been only able to consider the iron line alone due in part to a lack of adequate waveband coverage and / or good spectral resolution.

The improved S/N (as compared to GINGA) along with the high energy coverage afforded by RXTE coupled with simultaneous ASCA observations have allowed us not only to detect such features in our observations of MCG-6-30-15 but to set bounds on the abundances as a function of reflective fraction (figure 4) at the 95 per cent confidence level. This will have important consequences for understanding the geometry, and constraining processes in AGN central regions.

Acknowledgments. We thank all the members of the RXTE GOF for answering our inquiries in such a timely manner, with special thanks to William Heindl and the HEXTE team for help with HEXTE data reduction. We also thank Keith Jahoda for explanations of PCA calibration issues. JCL thanks the Isaac Newton Trust, the Overseas Research Studentship programme (ORS) and the Cambridge Commonwealth Trust for support. ACF thanks the Royal Society for support. CSR thanks the National Science Foundation for support under grant AST9529175, and NASA for support under the Long Term Space Astrophysics grant NASA-NAG-6337. KI and WNB thank PPARC and NASA RXTE grant NAG5-6852 for support, respectively.

References

- George, I. M. & Fabian, A. C. 1991, MNRAS, 249, 352
 Lee, J. C., Fabian, A. C., Reynolds, C. S., Iwasawa K., & Brandt, W. N. 1998, MNRAS, in press
 Lightman, A. & White, T. R. 1988, ApJ, 335, 57
 Magdziarz, P. & Zdziarski, A. 1995, MNRAS, 273, 837
 Nandra, K. & Pounds, K. A. 1994, MNRAS, 268, 405
 Reynolds, C. S. & Fabian, A. C., 1997. MNRAS, 290, L1
 Rees, M. J. 1984, ARA&A, 22, 471